

Covariant QCD Modeling of Light Meson Physics*

Peter C. Tandy†

Center for Nuclear Research, Department of Physics,
Kent State University, Kent, Ohio 44242 U.S.A.

(Dated: January 7, 2003)

We summarize recent progress in soft QCD modeling based on the set of Dyson–Schwinger equations truncated to ladder-rainbow level. This covariant approach to hadron physics accommodates quark confinement and implements the QCD one-loop renormalization group behavior. We compare the dressed quark propagator, pseudoscalar and vector meson masses as a function of quark mass, and the $\rho \rightarrow \pi\pi$ coupling to recent lattice-QCD data. The error in the Gell-Mann–Oakes–Renner relation with increasing quark mass is quantified by comparison to the exact pseudoscalar mass relation as evaluated within the ladder-rainbow Dyson-Schwinger model.

I. INTRODUCTION

The study of light-quark pseudoscalar and vector mesons is an important tool for understanding how QCD works in the non-perturbative regime. The pseudoscalars are important because they are the lightest observed hadrons and are the Goldstone bosons associated with dynamical chiral symmetry breaking. The ground state vector mesons are important because, as the lowest spin excitations of the pseudoscalars, they relate closely to hadronic $\bar{q}q$ modes that are electromagnetically excited.

We use a Poincaré covariant model defined within the framework of the Dyson–Schwinger equations [DSEs] of QCD; these form an excellent tool to study nonperturbative aspects of hadron properties [1]. It is straightforward to implement the correct one-loop renormalization group behavior of QCD [2], and obtain agreement with perturbation theory in the perturbative region. Provided that the relevant Ward–Takahashi identities are preserved in the truncation of the DSEs, the corresponding currents are conserved. Axial current conservation induces the Goldstone nature of the pions and kaons [3]; electromagnetic current conservation produces the correct electric charge of the mesons without fine-tuning. These properties are implemented here within the rainbow truncation of the DSE for the dressed quark propagators together with the ladder approximation for the Bethe–Salpeter equation [BSE] for meson bound states.

The model [4] we use has two infrared parameters which specify the momentum distribution and strength of the ladder-rainbow kernel at a low scale necessary to generate an empirically acceptable amount of dynamical chiral symmetry breaking [5, 6] as measured by the chiral condensate. As a corollary, the strong dressing of the quark propagator shifts the mass pole significantly away from the real timelike p^2 axis. The produced bound state mesons do not have a $\bar{q}q$ decay width and, in this sense, the present model implements quark confinement. The

absence of a real mass pole for dressed quark and gluon propagators has been studied and found to be a sufficient, but not necessary, condition for confinement [1, 7, 8, 9]. The model provides an efficient description of the masses and decay constants of the light-quark pseudoscalar and vector mesons [2, 4], the elastic charge form factors $F_\pi(Q^2)$ and $F_K(Q^2)$ [10] and the electroweak transition form factors of the pseudoscalars and vectors [11, 12].

II. DYSON-SCHWINGER EQUATIONS

The dressed quark propagator $S(p)$ is the solution to

$$S(p)^{-1} = Z_2 i \not{p} + Z_4 m(\mu) + Z_1 \int_q^\Lambda g^2 D_{\mu\nu}(p-q) \frac{\lambda^i}{2} \gamma_\mu S(q) \Gamma_\nu^i(q, p) \quad (1)$$

where $D_{\mu\nu}(k)$ is the renormalized dressed-gluon propagator, $\Gamma_\nu^i(q, p)$ is the renormalized dressed quark-gluon vertex. The notation $\int_q^\Lambda = \int d^4q / (2\pi)^4$ denotes a translationally invariant regularization of the integral with mass-scale Λ . The solution is renormalized according to $S(p)^{-1} = i\gamma \cdot p + m(\mu)$ at a sufficiently large spacelike μ^2 , with $m(\mu)$ the renormalized quark mass at the scale μ . The renormalization constants Z_2 and Z_4 depend on the renormalization mass-scale μ and on the regularization mass-scale Λ . The limit $\Lambda \rightarrow \infty$ is to be taken at the end of all calculations.

The BSE for a $a\bar{b}$ meson is

$$\Gamma^{a\bar{b}}(p_+, p_-) = \int_q^\Lambda K(p, q; P) S^a(q_+) \Gamma^{a\bar{b}}(q_+, q_-) S^b(q_-), \quad (2)$$

where K is the renormalized $q\bar{q}$ scattering kernel that is irreducible with respect to a pair of $q\bar{q}$ lines. The quark momenta are q_\pm ; the meson momentum is $P = q_+ - q_-$ and satisfies $P^2 = -m^2$. The relative momentum q is introduced by $q_+ = q + \eta P$ and $q_- = q - (1 - \eta)P$ where η is the momentum partitioning parameter. Physical observables should not depend on η and this provides a convenient check on numerical methods. We employ the model that has been developed recently for an efficient

*Presented at International School on Nuclear Physics, Erice, September 2002; to appear in Prog. Part. Nucl. Phys.

†tandy@cnr2.kent.edu

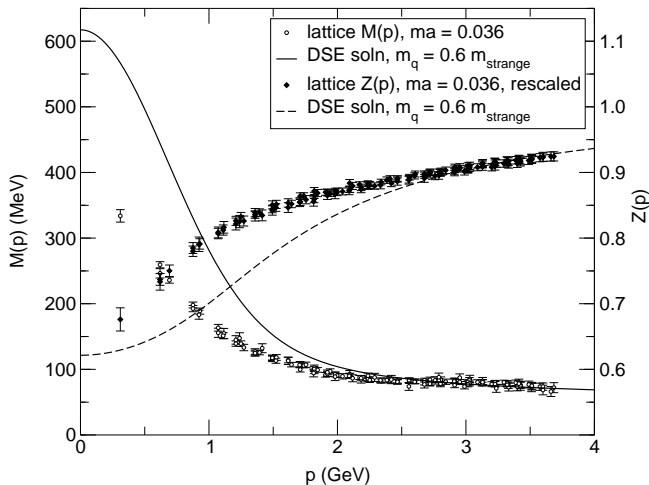


FIG. 1: DSE solution [4, 13] for quark propagator amplitudes compared to recent lattice data [14, 15].

description of the masses and decay constants of the light pseudoscalar and vector mesons [2, 4]. This consists of the rainbow truncation of the DSE for the quark propagator and the ladder truncation of the BSE for the pion and kaon amplitudes. The required effective $\bar{q}q$ interaction is constrained by perturbative QCD in the ultraviolet and has a phenomenological infrared behavior. In particular, the rainbow truncation of the quark DSE, Eq. (1), and the ladder truncation of the BSE, Eq. (2), are

$$Z_1 g^2 D_{\mu\nu}(k) \Gamma_\nu^i(q, p) \rightarrow 4\pi \alpha_{\text{eff}}(k^2) D_{\mu\nu}^{\text{free}}(k) \gamma_\nu \frac{\lambda^i}{2}, \quad (3)$$

and

$$K(p, q; P) \rightarrow -4\pi \alpha_{\text{eff}}(k^2) D_{\mu\nu}^{\text{free}}(k) \frac{\lambda^i}{2} \gamma_\mu \otimes \frac{\lambda^i}{2} \gamma_\nu, \quad (4)$$

where $D_{\mu\nu}^{\text{free}}(k = p - q)$ is the free gluon propagator in Landau gauge. These two truncations are consistent in the sense that the combination produces vector and axial-vector vertices satisfying the respective WTIs. In the axial case, this ensures that in the chiral limit the ground state pseudoscalar mesons are the massless Goldstone bosons associated with chiral symmetry breaking [2, 3]. In the vector case, this ensures electromagnetic current conservation. The “effective coupling” $\alpha_{\text{eff}}(k^2)$ defines the model. The ultraviolet behavior is chosen to be that of the QCD running coupling $\alpha(k^2)$; the ladder-rainbow truncation then generates the correct perturbative QCD structure of the DSE-BSE system of equations. The phenomenological infrared form of $\alpha_{\text{eff}}(k^2)$ is chosen so that the DSE kernel contains sufficient infrared enhancement to produce an empirically acceptable amount of dynamical chiral symmetry breaking as represented by the chiral condensate [18].

We employ the Ansatz found to be successful in earlier

TABLE I: The pseudoscalar observables that define the present ladder-rainbow DSE-BSE model, adapted from Refs. [2, 4].

	experiment (estimates)	calculated ([†] fitted)
$m_{\mu=1\text{GeV}}^{u=d}$	5 - 10 MeV	5.5 MeV
$m_{\mu=1\text{GeV}}^s$	100 - 300 MeV	125 MeV
$-\langle \bar{q}q \rangle_\mu^0$	$(0.236 \text{ GeV})^3$	$(0.241^\dagger)^3$
m_π	0.1385 GeV	0.138 [†]
f_π	0.131 GeV	0.131 [†]
m_K	0.496 GeV	0.497 [†]
f_K	0.160 GeV	0.155

work [2, 4]

$$\frac{\mathcal{G}(k^2)}{k^2} = \frac{4\pi^2 D k^2}{\omega^6} e^{-k^2/\omega^2} + \frac{4\pi^2 \gamma_m \mathcal{F}(k^2)}{\frac{1}{2} \ln \left[\tau + \left(1 + k^2/\Lambda_{\text{QCD}}^2 \right)^2 \right]}, \quad (5)$$

with $\gamma_m = \frac{12}{33-2N_f}$ and $\mathcal{F}(s) = (1 - \exp(-\frac{s}{4m_t^2}))/s$. The first term implements the strong infrared enhancement in the region $0 < k^2 < 1 \text{ GeV}^2$ required for sufficient dynamical chiral symmetry breaking. The second term serves to preserve the one-loop renormalization group behavior of QCD. We use $m_t = 0.5 \text{ GeV}$, $\tau = e^2 - 1$, $N_f = 4$, and we take $\Lambda_{\text{QCD}} = 0.234 \text{ GeV}$. The renormalization scale is chosen to be $\mu = 19 \text{ GeV}$ which is well into the domain where one-loop perturbative behavior is appropriate [2, 4]. The remaining parameters, $\omega = 0.4 \text{ GeV}$ and $D = 0.93 \text{ GeV}^2$ along with the quark masses, are fitted to give a good description of $\langle \bar{q}q \rangle$, $m_{\pi/K}$ and f_π as shown in Table I. The subsequent values for f_K and the masses and decay constants of the vector mesons ρ , ϕ , K^* are found to be within 10% of the experimental data [4].

In Fig. 1 we compare the DSE model propagator amplitudes defined by $S(p) = Z(p^2)[i\not{p} + M(p^2)]^{-1}$ with the most recent results in lattice QCD using staggered fermions in Landau gauge [14, 15]. These simulations were done with the Asqtad improved staggered quark action, which has lattice errors of order $\mathcal{O}(a^4)$ and $\mathcal{O}(a^2 g^2)$. Fig. 1 shows both $M(p)$ and $Z(p)$ obtained with a bare lattice mass of $ma = 0.036$ in lattice units, which corresponds to a bare mass of 57 MeV in physical units. The DSE calculations use a current mass value of 75 MeV at $\mu = 1 \text{ GeV}$ to match the lattice mass function around 3 GeV; this current mass is about $0.6 m_s$. There is agreement in the qualitative infrared structure of $M(p)$ and $Z(p)$. Since the lattice simulation produces the regulated but un-renormalized propagator, the scale of $Z(p)$ is arbitrary and we have rescaled the lattice $Z(p)$ to match the DSE solution at 3 GeV. For $Z(p)$ the ladder-rainbow DSE model saturates much slower than does the lattice; this may signal a deficiency of the bare gluon-quark vertex. A recent study of the coupled ghost-gluon-quark DSEs has

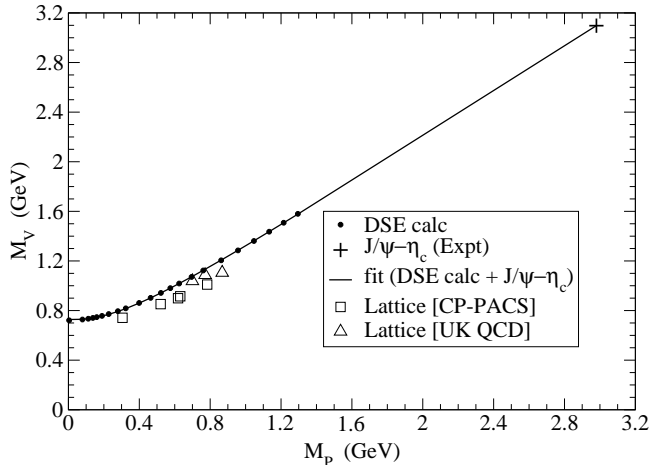


FIG. 2: DSE calculation of equal flavor vector meson mass variation with pseudoscalar meson mass as m_q is varied compared to lattice data from CP-PACS [16] and UK-QCD [17].

found that the quark-gluon vertex dressing can produce a change of this character in the infrared structure of the quark amplitudes [19, 20].

In Fig. 2 we compare the rainbow-ladder DSE model with unquenched lattice data for the variation of vector and pseudoscalar meson masses with quark current mass in the case of equal flavor quarks. The DSE calculation, shown by the discrete circles, is limited to the mass range where it is reliable. The solid line is a fit to those results plus the experimental $J/\psi - \eta_c$ point. The curvature at low mass is consistent with $M_V \propto m_q$ and $M_P \propto \sqrt{m_q}$. This comparison is consistent with the known properties of the DSE results: M_V is 5% too low for the ρ and 5% too high for the ϕ , while the pseudoscalar masses in the u -quark and s -quark regions are fit to experiment. (If the evident fit is continued to the Υ vector mass, the predicted η_b mass would be 10.0 GeV.)

III. PSEUDOSCALAR MESON MASS RELATION

As the current quark mass is raised from zero, the explicit breaking of chiral symmetry adds mass to the Goldstone boson modes. The way in which the pseudoscalar meson mass grows with quark mass is described, at low mass, by the GMOR relation. This is

$$M_P^2(m_1(\mu), m_2(\mu)) = [m_1(\mu) + m_2(\mu)] \frac{|\langle \bar{q}q \rangle_\mu^0|}{(f_P^0)^2} + \mathcal{O}(m^2), \quad (6)$$

in the general case where the two quark flavors are different. Here $\langle \bar{q}q \rangle_\mu^0 = -Z_4 N_c \text{tr} \int_q^\Lambda S_0(q)$ is the chiral con-

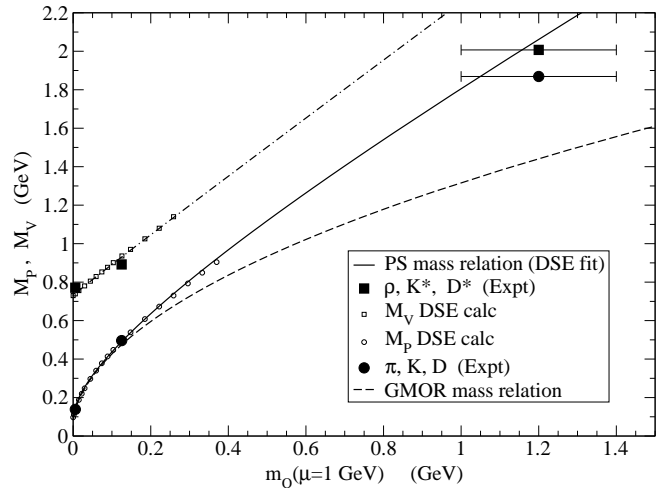


FIG. 3: $M_V(m_Q)$ and $M_P(m_Q)$ for unequal flavor $u - Q$ mesons. The DSE model-exact mass relation reveals the size of the correction to the GMOR relation.

densate at scale μ , the current masses are determined at the same scale, and f_P^0 is the chiral limit electroweak decay constant (in the $f_\pi = 92.4$ MeV convention). For u/d quarks the GMOR relation is satisfied to high accuracy (within 0.2% in the present DSE model). For current masses of the order of $m_s \sim 120$ MeV and above, the question of the size of the error in the GMOR relation is not settled. An exact mass relation for pseudoscalar

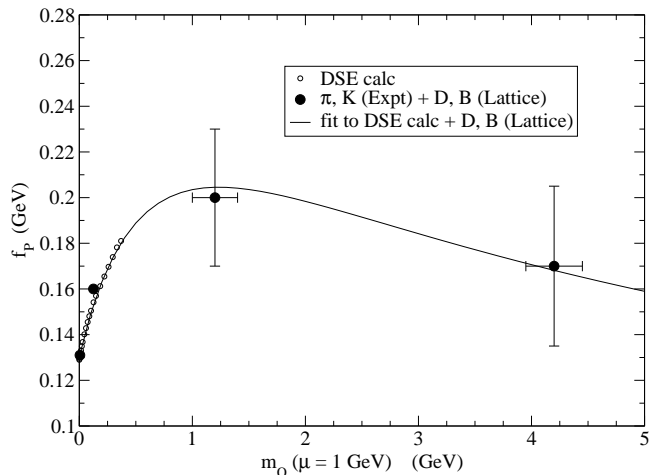


FIG. 4: Current quark mass dependence of f_P , the electroweak decay constant for $u - Q$ mesons. [$f_\pi = 131$ MeV convention.]

mesons in QCD, applicable for all values of the quark masses, has been established [3]. With allowance for different quark flavors, it takes the form

$$M_P^2 f_P(m_1, m_2) = (m_1 + m_2) R_P(m_1, m_2), \quad (7)$$

where R_P is the projection of the meson wave function onto γ_5 at the origin of $\bar{q}q$ separation and is given by [3]

$$R_P = -i Z_4 N_c \int_q^\Lambda \text{tr}[\gamma_5 S_{f_1}(q_+) \Gamma_P(q; P) S_{f_2}(q_-)], \quad (8)$$

with all renormalized quantities taken at the same scale μ . The chiral limit of this quantity can be shown to be $R_P(m_1 = m_2 = 0) = -\langle \bar{q}q \rangle_\mu^0 / f_P^0$, and thus the GMOR relation follows as a corollary of the exact relation, Eq. (7), at low mass. The origin of this exact mass relation is the axial vector Ward-Takahashi relation

$$\begin{aligned} -i P_\mu \Gamma_{5\mu}(q; P) &= S_{f_1}^{-1}(q_+) \gamma_5 + \gamma_5 S_{f_2}^{-1}(q_-) \\ &\quad - (m_1 + m_2) \Gamma_5(q; P) . \end{aligned} \quad (9)$$

The dressed vertices $\Gamma_{5\mu}(q; P)$ and $\Gamma_5(q; P)$ satisfy inhomogeneous integral equations that have the same kernel, the irreducible $\bar{q}q$ scattering amplitude; the inhomogeneous terms are $Z_2 \gamma_\mu$ and $Z_4 \gamma_5$ respectively. Thus both vertices have poles corresponding to the pseudoscalar meson bound states. [The axial vector poles in $\Gamma_{5\mu}$ have transverse residues and do not contribute.] The exact mass relation, Eq. (7), arises from the equality of the pseudoscalar pole residues from both sides of Eq. (9). The residue of $\Gamma_5(q; P)$ is $-i R_P \Gamma_P(q; P)$, and the residue of $\Gamma_{5\mu}(q; P)$ is $P_\mu f_P \Gamma_P(q; P)$, where Γ_P is the pseudoscalar bound state BS amplitude. The expression for $f_P P_\mu$ is the same as for R_P in Eq. (8) except that γ_5 is replaced by $\gamma_5 \gamma_\mu$ and $-i Z_4$ is replaced by $Z_2 / \sqrt{2}$ (in the convention where the physical f_π is 92.4 MeV). In the chiral limit, the last term of Eq. (9)

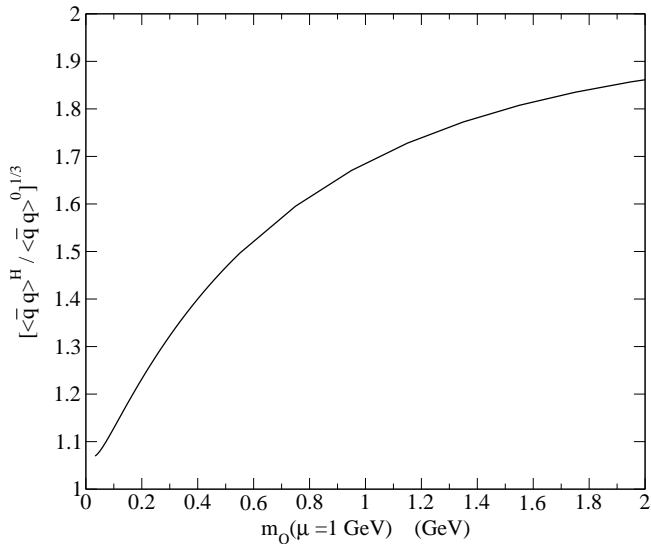


FIG. 5: A measure of the current quark mass dependence of the in-hadron condensate for qQ pseudoscalars.

is not present and the right hand side is not singular. A systematic expansion in powers of P_μ reveals [3] that in leading order the pole in the left hand side must move to

$P^2 = 0$ to be cancelled and thus $M_P = 0$. The analysis also provides relationships between the BS amplitude and the quark propagator, e.g., $f_P^0 E_P^0(q; 0) = B_0(q^2)$, where $\Gamma_P(q; P) = i\gamma_5 E_P + \dots$. Since the quark mass function is proportional to $B_0(q^2)$, this latter relation means that dynamical chiral symmetry breaking is necessarily accompanied by a massless pseudoscalar bound state. This is the familiar Goldstone's theorem; notice that the composite, distributed nature of the pion amplitude requires a running quark mass function.

At small m , both f_P and R_P are constant leading to the GMOR behavior $M_P \sim \sqrt{m}$. The error in this has to increase with mass since the heavy quark limiting behavior is [21] $f_P \sim 1/\sqrt{m}$ and $R_P \sim \sqrt{m}$ which leads to the linear behavior $M_P \sim m$.

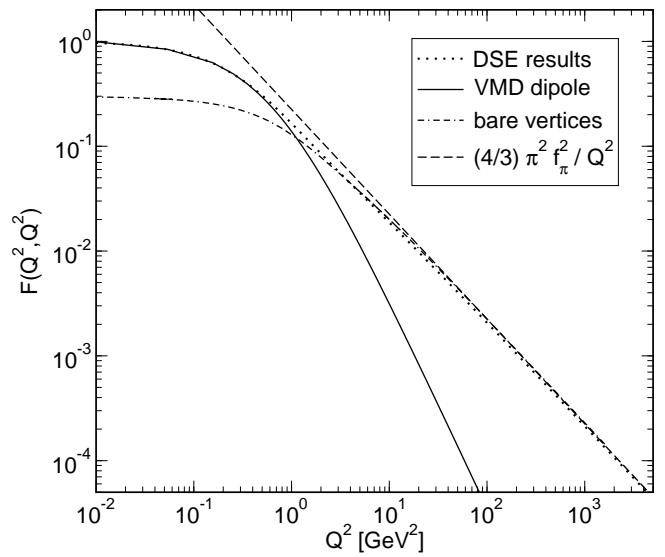


FIG. 6: Our DSE results for the symmetric $\gamma^* \pi \rightarrow \gamma^*$ form factor, compared to the pQCD asymptotic $1/Q^2$ behavior. [Here $f_\pi = 131$ MeV.] The naive VMD model suggests a dipole behavior which is correct only in the infrared.

The evolution of both vector and pseudoscalar meson masses with increasing current quark mass has been studied within the DSE model in both the equal and unequal flavor cases. An example is shown in Fig. 3 for $u - Q$ mesons as a function of $m_Q(\mu = 1 \text{ GeV})$ up to the limit of accuracy of the calculations. The fit shown is adapted from Ref. [22] by evolving the $m_Q(\mu = 19 \text{ GeV})$ used there to $\mu = 1 \text{ GeV}$ for ease of comparison with conventionally quoted values. Thus here we have $M_P = \alpha' + \beta' \sqrt{m_Q} + \gamma' m_Q$; with both masses in GeV, the parameters are $(\alpha', \beta', \gamma') = (0.083, 0.842, 0.880)$. With the DSE model-exact values of f_P^0 and $\langle \bar{q}q \rangle_\mu^0$, the GMOR relation is explicitly $M_P^2 = 0.00955 + 1.724 m_Q(\mu = 1 \text{ GeV})$ and this is compared to the exact mass relation in Fig. 3. For the K meson the GMOR error is 4%, at $m_Q = 0.4 \text{ GeV}$ the error is 14%, while at the D meson the error is 30%. In the D meson region, only $\sim 50\%$ of the mass comes from the linear term; the heavy quark domain is at higher

TABLE II: The coupling constants $g_{v \rightarrow pp}$ calculated in the DSE model compared to results from a fit to the timelike form factor pole [24, 25] and lattice-QCD [26].

$g_{v \rightarrow pp}$	Expt	this work	pole fit	lattice-QCD
$g_{\rho \rightarrow \pi\pi}$	6.02	5.14	5.2	$6.08^{+2.04}_{-1.00}$
$g_{\phi \rightarrow KK}$	4.64	4.25	4.3	-
$g_{K^* \rightarrow K^0 \pi^+}$	4.60	4.81	4.1	-

mass.

The exact mass relation $M_P(m_Q)$, Eq. (7), differs from the GMOR behavior due to the mass dependence of f_P and R_P . Instead of the latter quantity, one can define $\langle \bar{q}q \rangle_\mu^H = -f_P R_P$ as an effective “in-hadron” condensate [21] which allows the exact mass relation to take the GMOR-like form $M_P^2 f_P^2 = (m_1 + m_2)_\mu |\langle \bar{q}q \rangle_\mu^H|$. From this relation we extract the quark mass dependence of $\langle \bar{q}q \rangle_\mu^H$ at $\mu = 1$ GeV. The low mass DSE results for M_P and f_P are fitted to forms that respect the heavy quark limits, are consistent with D and B meson masses, and are consistent with lattice results [23] for f_P of the D and B mesons. We adapt the $f_P(M_P)$ fit from Ref. [21] to produce $f_P(m_Q)$ and to accommodate the DSE results at low mass. The result is displayed in Fig. 4. The fit (in the $f_\pi = 131$ MeV convention) is $f_P^2 = N/D$, where $N = a + b m_Q$ and $D = 1.0 + c m_Q + d m_Q^2$, with $(a, b, c, d) = (0.017, 0.068, 0.649, 0.391)$ when m_Q is in GeV. The resulting estimate of the mass dependence for $\langle \bar{q}q \rangle_\mu^H$ at $\mu = 1$ GeV is shown in Fig. 5 and indicates $\sim 15\%$ increase over the chiral limit value for an m_Q relevant to K , while for the D meson the in-hadron condensate is about 70% enhanced.

IV. VECTOR MESON STRONG DECAYS

Since this DSE model describes the elastic charge form factors of the pseudoscalars very well [10] in impulse approximation, the strong decays of the vector mesons should be well-described without parameter adjustment. In impulse approximation, the amplitude for the decay of ρ with 4-momentum $Q = p_1 + p_2$ to $\pi\pi$ with 4-momenta p_1, p_2 is given by [13]

$$2P_\mu^T g_{\rho \rightarrow \pi\pi} = \sqrt{2} N_c \text{tr} \int_k^\Lambda S(q) \Gamma_P(q, q_+) S(q_+) \times \Gamma_\mu(q_+, q_-) S(q_-) \bar{\Gamma}_P(q_-, q), \quad (10)$$

where no distinction is made between the u/d quarks, $P = (p_1 - p_2)/2$, $q = k + P/2$ and $q_\pm = k - P/2 \pm Q/2$. The appropriate generalizations of the flavor structure appropriate to $\phi \rightarrow KK$ and $K^* \rightarrow K\pi$ are straightforward [13]. In Eq. (10), the component of P_μ transverse to Q_μ is indicated on the left hand side to cover the case of unequal decay products.

The results shown in Table II are within 5-10% of experiment with the error being larger if the vector meson

is lighter. As an independent check, coupling constants are also extracted from the timelike electroweak form factors near the vector meson poles [24, 25]. The agreement is encouraging considering that with eight independent covariants for the vector BS amplitude and four each for the pseudoscalars, there are 128 distinct quark loop integrals for each physical decay. Also shown in Table II is a recent lattice-QCD result [26] for $\rho \rightarrow \pi\pi$ from the UKQCD Collaboration. Although the lattice data is at $m_\pi/m_\rho = 0.578$, which corresponds to the s -quark mass, and thus no physical decay of the ρ can take place, the amplitude $\langle \rho | \pi\pi \rangle$ is accessible through study of state mixing on the lattice.

Since the width of the ρ is almost 20% of its mass while the widths of the ϕ and K^* are significantly less important, we expect the ladder approximation for the BSE kernel (which omits the strong channels $\pi\pi$, KK and $K\pi$ respectively) to be less accurate for the ρ than for the ϕ and K^* . Accordingly we speculate that this is largely the reason why the result for $g_{\rho \rightarrow \pi\pi}$ in Table II deviates from experiment twice as much (15%) as do the other decay constants.

V. PQCD LIMIT OF FORM FACTORS

Besides the soft physical characteristics of light mesons, the present DSE model should also reproduce perturbative QCD limits. This has been checked for the uv behavior of the quark mass function $M(p^2)$; both the leading log behavior away from the chiral limit, and the coefficient of the leading $1/p^2$ behavior in the chiral limit reproduce the exact 1-loop results of QCD [2]. A more difficult task is to test the asymptotic behavior of meson form factors against pQCD predictions. This is complicated by the fact that covariant ladder-rainbow calculations that link the dressed quark propagator, the BSE, and the impulse approximation for form factors have only been carried out in Euclidean metric for practical reasons. The mass-shell constraint for mesons then requires an analytic continuation which entails complex quark momenta in loop integrals. This greatly hinders the asymptotic analysis.

A case that is free of these difficulties is the symmetric $\gamma^* \pi \rightarrow \gamma^*$ transition where the photons are taken to have equal virtuality Q^2 and there is only one mass-shell constraint. Since m_π^2 is negligible compared to all other scales in the problem, all involved quark momenta are essentially real and spacelike. In Fig. 6 we show the result [11] of the present DSE model compared to the pQCD asymptotic behavior [27] obtained from the light-cone operator product expansion. (In this case, log corrections occur at sub-leading order.) The numerically generated asymptotic behavior of the DSE-based model reproduces the pQCD limit as it must. By about 2 GeV^2 the dressing of the photon vertices becomes negligible; however the 3-point function does not become an effective 2-point function (thereby generating the required power

of f_π) until about 15-20 GeV² [11]. Such a high scale for the onset of pQCD behavior is consistent with an earlier observation [28] in a DSE-based model study of $F_\pi(Q^2)$.

VI. DISCUSSION

Recent reviews [1, 29] put this model in a wider perspective and compile results for both meson and baryon physics, an analysis how quark confinement is manifest in solutions of the DSEs, and both finite temperature and finite density extensions. The question of the relevance and accuracy of the ladder-rainbow truncation has also received some attention; it has been shown to be particularly suitable for the flavor octet pseudoscalar mesons since the next-order contributions to the BSE kernel, in a quark-gluon skeleton graph expansion, have a significant

amount of cancellation between repulsive and attractive corrections [30, 31]. The preservation of the axial vector WTI is what makes the pseudoscalar meson sector a robust and ideal base for parameter fixing; the rainbow-ladder truncation may be used as a convenience in that sector. It is hoped that future interplay between lattice simulations and continuum modeling will increase our understanding of QCD for hadron physics.

Acknowledgments

Thanks are due A. Faessler and T. Gutsche for organization of a stimulating school in Erice. Very helpful comments from Pieter Maris are acknowledged. This work was supported in part by NSF grants No. PHY-0071361 and INT-0129236.

-
- [1] C. D. Roberts and S. M. Schmidt, *Prog. Part. Nucl. Phys.* **45S1**, 1 (2000), nucl-th/0005064.
 - [2] P. Maris and C. D. Roberts, *Phys. Rev.* **C56**, 3369 (1997), nucl-th/9708029.
 - [3] P. Maris, C. D. Roberts, and P. C. Tandy, *Phys. Lett.* **B420**, 267 (1998), nucl-th/9707003.
 - [4] P. Maris and P. C. Tandy, *Phys. Rev.* **C60**, 055214 (1999), nucl-th/9905056.
 - [5] D. Atkinson and P. W. Johnson, *Phys. Rev.* **D37**, 2296 (1988).
 - [6] C. D. Roberts and B. H. J. McKellar, *Phys. Rev.* **D41**, 672 (1990).
 - [7] C. J. Burden, C. D. Roberts, and A. G. Williams, *Phys. Lett.* **B285**, 347 (1992).
 - [8] G. Krein, C. D. Roberts, and A. G. Williams, *Int. J. Mod. Phys.* **A7**, 5607 (1992).
 - [9] P. Maris, *Phys. Rev.* **D52**, 6087 (1995), hep-ph/9508323.
 - [10] P. Maris and P. C. Tandy, *Phys. Rev.* **C62**, 055204 (2000), nucl-th/0005015.
 - [11] P. Maris and P. C. Tandy, *Phys. Rev.* **C65**, 045211 (2002), nucl-th/0201017.
 - [12] C.-R. Ji and P. Maris, *Phys. Rev.* **D64**, 014032 (2001), nucl-th/0102057.
 - [13] D. Jarecke, P. Maris, and P. C. Tandy (2002), nucl-th/0208019.
 - [14] P. O. Bowman, U. M. Heller, and A. G. Williams, *Phys. Rev.* **D66**, 014505 (2002), hep-lat/0203001.
 - [15] P. Bowman (2002), private communication.
 - [16] S. Aoki et al. (CP-PACS), *Phys. Rev.* **D60**, 114508 (1999), hep-lat/9902018.
 - [17] C. R. Allton et al. (UKQCD), *Phys. Rev.* **D60**, 034507 (1999), hep-lat/9808016.
 - [18] F. T. Hawes, P. Maris, and C. D. Roberts, *Phys. Lett.* **B440**, 353 (1998), nucl-th/9807056.
 - [19] C. S. Fischer (2002), PhD Thesis, University of Tuebingen, unpublished.
 - [20] R. Alkofer (2002), private communication.
 - [21] M. A. Ivanov, Y. L. Kalinovsky, and C. D. Roberts, *Phys. Rev.* **D60**, 034018 (1999), nucl-th/9812063.
 - [22] P. Maris (2000), nucl-th/0009064.
 - [23] J. M. Flynn and C. T. Sachrajda, *Adv. Ser. Direct. High Energy Phys.* **15**, 402 (1998), hep-lat/9710057.
 - [24] P. Maris and P. C. Tandy, *Mesons as Bound States of Confined Quarks: Zero and Finite Temperature*, for the proceedings of Research Program at the Erwin Schodinger Institute on Confinement, Vienna, Austria, 5 May - 17 Jul 2000, (2001), nucl-th/0109035.
 - [25] P. Maris (2001), nucl-th/0112022.
 - [26] C. McNeile and C. Michael (UKQCD) (2002), hep-lat/0212020.
 - [27] G. P. Lepage and S. J. Brodsky, *Phys. Rev.* **D22**, 2157 (1980).
 - [28] P. Maris and C. D. Roberts, *Phys. Rev.* **C58**, 3659 (1998), nucl-th/9804062.
 - [29] R. Alkofer and L. von Smekal, *Phys. Rept.* **353**, 281 (2001), hep-ph/0007355.
 - [30] A. Bender, C. D. Roberts, and L. Von Smekal, *Phys. Lett.* **B380**, 7 (1996), nucl-th/9602012.
 - [31] A. Bender, W. Detmold, C. D. Roberts, and A. W. Thomas, *Phys. Rev.* **C65**, 065203 (2002), nucl-th/0202082.